

Exploring new opportunities with sum-frequency nonlinear optical spectroscopy*

Y. R. Shen

Department of Physics, University of California, Berkeley, CA 94720, USA

Abstract: Over the last decade, infrared-visible sum-frequency generation has been developed into a powerful vibrational spectroscopic technique, especially for surface studies. We give here a brief review of the technique and a few recent applications of the technique to liquid and polymer surfaces. We also describe how the technique has found unique applications in our studies of surface melting of ice, ferroelectric ice films, and molecular chirality in chiral liquids. Doubly resonant sum-frequency generation as surface-specific two-dimensional spectroscopy is discussed.

INTRODUCTION

The advent of laser has led to the invention of many powerful nonlinear optical spectroscopic techniques. Among them, sum-frequency generation (SFG) spectroscopy has recently received much attention. SFG is a process in which two input beams at frequencies ω_1 and ω_2 mix in a medium and generate an output beam at the sum frequency $\omega = \omega_1 + \omega_2$ [1]. As a second-order nonlinear optical process, it is only allowed under electric-dipole approximation in media without inversion symmetry. At surfaces or interfaces where inversion symmetry is necessarily broken, SFG is naturally allowed even in media with inversion symmetry and can therefore be used as an effective surface probe for such media [2]. If either ω_1 (ω_2) or $\omega_1 + \omega_2$ or both are scanned over resonances, SFG should be resonantly enhanced and thus yield an SF spectrum for the medium.

SFG can be used to probe electronic as well as vibrational transitions in a medium. For molecular systems, however, vibrational spectroscopy is often more selective. As shown in Fig. 1a, SFG vibrational spectroscopy requires a tunable infrared input beam (ω_2) for scanning over vibrational resonances. In contrast to infrared and Raman spectroscopy, SFG probes only vibrational modes that are both infrared and Raman active. But most importantly, unlike infrared and Raman spectroscopy, SFG is surface-specific in media with inversion symmetry.

As a surface vibrational spectroscopy, SFG has many characteristic merits. It has enough sensitivity to probe a submonolayer of molecules. Since the process is coherent, the output is highly directional. It can therefore be used for *in situ* remote sensing of a surface even in hostile environment. As a laser spectroscopy technique, it is capable of high spectral, spatial, and temporal resolution. Finally, above all, it is a technique applicable to all interfaces accessible by light. Consequently, it has found many unique applications over the years. Among them are studies of liquid interfaces, polymer interfaces, buried interfaces, surface reactions under real atmosphere, surface dynamics, and many others. We describe here as examples a few recent experiments performed in our laboratory. With both inputs tunable, SFG can experience doubly resonant enhancement [3]. The resultant two-dimensional spectroscopy is far more selective than the singly resonant SFG, as in the case of resonant Raman spec-

*Lecture presented at the IUPAC International Congress on Analytical Sciences 2001 (ICAS2001), Tokyo, Japan, 6–10 August 2001. Other presentations are published in this issue, pp. 1555–1623.

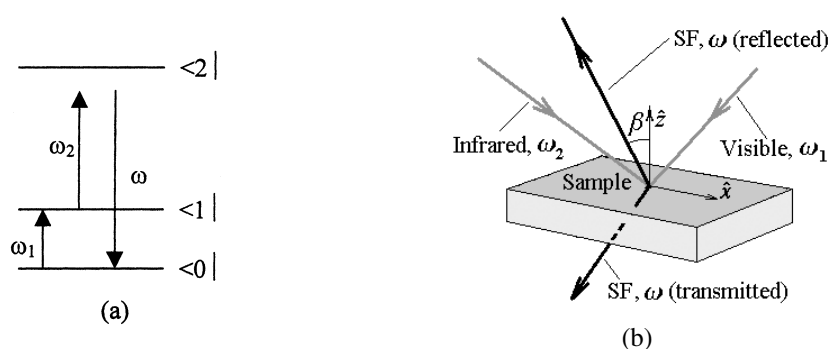


Fig. 1 Schematic diagram describing (a) the SFG process and beam geometry for SFG in the transmission and reflection directions.

troscopy. Unlike resonant Raman spectroscopy, however, doubly resonant SFG is surface-specific and applicable even to media that strongly fluoresce. We discuss briefly a recent experiment that demonstrates the technique.

SFG spectroscopy can be employed to study bulk materials as well. We describe also in this paper two intriguing cases where the technique has helped. One is on the discovery of ferroelectric ice, and the other on probing vibrational chirality of liquid.

THEORETICAL BACKGROUND

For convenience of later discussion, we give here a brief account of the basic theory underlying the SFG process. The details can be found elsewhere [1]. Under the electric-dipole approximation, SFG is generated from a second-order nonlinear polarization

$$P_i^{(2)}(\omega) = \chi_{ijk}^{(2)}(\omega = \omega_1 + \omega_2) E_j(\omega_1) E_k(\omega_2) \quad (1)$$

induced in a medium. Structural symmetry of the medium makes a certain number of the 27 nonlinear susceptibility elements $\chi_{ijk}^{(2)}$ vanish or dependent of one another. In particular, for a medium with inversion symmetry, $\chi_{ijk}^{(2)}$ for the bulk must all vanish. The nonlinear susceptibility $\chi^{(2)}$ is related to the nonlinear polarizability $\alpha^{(2)}$ of molecules by

$$\chi_{ijk}^{(2)} = N \sum_{\lambda, \mu, \nu} \langle (\hat{i} \cdot \hat{\lambda})(\hat{j} \cdot \hat{\mu})(\hat{k} \cdot \hat{\nu}) \rangle \alpha_{\lambda\mu\nu}^{(2)} \quad (2)$$

with N denoting the bulk or surface density of molecules depending on whether $\chi_{ijk}^{(2)}$ refers to the bulk or surface nonlinear susceptibility. Here, for simplicity, we have neglected the microscopic local field correction on $\chi_{ijk}^{(2)}$.

Near vibrational resonances, $\alpha^{(2)}$ and $\chi^{(2)}$ can be written as

$$\alpha_{\lambda\mu\nu}^{(2)} = (\alpha_{NR}^{(2)})_{\lambda\mu\nu} + \sum_q \frac{(a_q)_{\lambda\mu\nu}}{\omega_2 - \omega_q + i\Gamma_q} \quad (3)$$

$$\chi_{ijk}^{(2)} = (\chi_{NR}^{(2)})_{ijk} + \sum_q \frac{(A_q)_{ijk}}{\omega_2 - \omega_q + i\Gamma_q}$$

where the subindex NR refers to the nonresonant background, ω_q and Γ_q are the resonant frequency and damping coefficient of the q th vibrational mode, and the mode strengths a_q and A_q are related similarly as $\alpha^{(2)}$ and $\chi^{(2)}$ in eq. 2.

In spectroscopic applications, the resonant SFG output can often be described by

$$S \propto |\chi_{\text{eff}}^{(2)}|^2 |E(\omega_1)|^2 |E(\omega_2)|^2 \quad (4)$$

with $\chi_{\text{eff}}^{(2)} = F(\hat{e}, \hat{e}_1, \hat{e}_2)[\hat{e} \cdot \tilde{\chi}^{(2)} : \hat{e}_1 \hat{e}_2]$

where the unit vector \hat{e}_i specifies the polarization of the field $E(\omega_i)$, and $F(\hat{e}, \hat{e}_1, \hat{e}_2)$ denotes the overall Fresnel coefficient for transmission and/or reflection at boundary surfaces. Equation 4 together with eq. 3 is generally used to fit the experimentally observed spectrum for a given input/output polarization combination and find $[\hat{e} \cdot \tilde{\chi}^{(2)} : \hat{e}_1 \hat{e}_2]$, from which $\chi_{ijk}^{(2)}$ hopefully can be determined. Knowing $\chi_{ijk}^{(2)}$, the structural information of the medium can be deduced. For example, from $\chi_{ijk}^{(2)}$ for a surface layer, information about the orientation of molecules at the surface can be extracted, as we shall see later in some examples.

EXPERIMENTAL ARRANGEMENT

The experimental arrangement for SFG spectroscopy is schematically described in Fig. 1b. In our experiments, the input beams are derived from a combined picosecond Nd:YAG laser/optical parametric system. Both the visible beam at ω_1 and the infrared beam at ω_2 are tunable, but for singly resonant vibrational spectroscopy, ω_1 is usually held fixed. The SF output appears in both transmission and reflection. The reflection geometry is generally used in surface studies. Since the output is monochromatic and highly directional, spatial and spectral filtering can be employed to discriminate against the background noise due to light scattering and induced fluorescence. The SF signal is finally detected by a photomultiplier connected to a gated integrator and a computer. For selection of input/output polarization combination, polarizers are inserted in the optical path before and after the sample. Detailed descriptions of our laser system and experimental setup have been reported elsewhere [1].

APPLICATIONS

Liquid interfaces

One of the unique applications of SFG vibrational spectroscopy (SFG-VS) is on neat liquid interfaces [4]. Interfacial properties of liquids are important owing to relevance in many reactions such as wetting, electrochemical reactions, and biological functions. The asymmetric environment of a liquid surface makes the interfacial properties significantly different from those of the isotropic bulk. Numerous theoretical studies in recent years have significantly enhanced our understanding of liquid interfaces at the microscopic level, but corresponding experimental investigations are still rare. Through determination of surface molecular orientations, SFG-VS has turned out to be a powerful tool for studies of liquid interfaces. As an example, we present here our recent work on the acetone/vapor interface [5].

Figure 2 depicts the SFG vibrational spectra of the acetone[(CH₃)₂-CO]/vapor interface in the CH stretch region taken with three different input/output polarization combinations. While three CH₃ modes, symmetric stretch, antisymmetric stretch, and Fermi resonance, are expected in this region, only the symmetric stretch is clearly observed, most prominently in the SSP (S-, S- and P-polarized SF output, visible input and infrared input, respectively) polarization combination.

This suggests that one of the two CH₃ groups of acetone projects out of the surface at a slanted angle (with an orientational distribution). SFG-VS in the CO stretch region was also measured, but no CO stretch mode was detected, indicating that the CO group of acetone lies close to the surface plane. The deduced orientation is similar to that of acetone molecules in a layer plane of the crystalline structure of acetone. Together with the known appreciable surface tension of acetone, we can then conclude that the acetone liquid surface has a more ordered structure than the bulk and is crystal-like. This con-

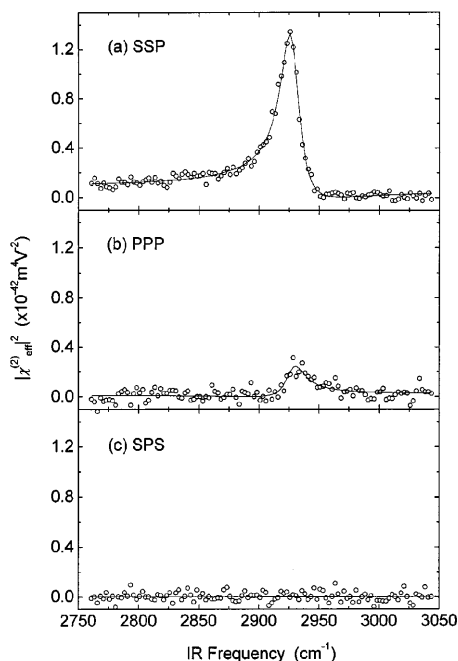


Fig. 2 Reflective SFG spectra of the liquid/vapor interface of acetone in the CH stretch region measured with three different polarization combinations: (a) SSP, (b) PPP, and (c) SPS. (After ref. 5.)

clusion has been substantiated by molecular dynamics calculation. We have obtained the same conclusion for other liquids that possess an appreciable surface tension.

Polymer interfaces

Polymer surfaces and interfaces play an important role in modern science and technology. Their properties are usually governed by surface structure and composition that can be very different from the bulk. For advances of polymer surface science, we would like to characterize polymer surfaces at the molecular level. Work in this respect, however, has been quite limited because few existing techniques are suitable for such tasks. SFG-VS appears to be among the most effective. It has been successfully applied to many polymer surfaces and interfaces including those of polyethylene, polyimides, biopolymers, and others [6]. We consider here a rubbed polyvinyl alcohol surface [PVA, $(-\text{CH}_2-\text{CHOH}-)$] as an example [7].

It is believed that rubbing of a polymer surface would induce alignment of main chains at the polymer surface [8]. Figure 3 presents the SFG vibrational spectra of the PVA/air interface with three input/output polarization combinations.

For the incidence plane parallel ($\gamma = 0^\circ$) and perpendicular ($\gamma = 90^\circ$) to the rubbing direction, the spectra are obviously different, exhibiting a strong anisotropy induced by rubbing. They can be well fit by eqs. 3 and 4 with three vibrational modes, the CH stretch at 2882 cm^{-1} , the CH_2 symmetric(s) stretch at 2907 cm^{-1} , and the antisymmetric(a) CH_2 stretch at 2940 cm^{-1} . The CH_2 s-mode is very weak in the SPS spectra. This is actually true for all sample orientations (specified by γ). Since excitation of the s-mode requires an infrared polarization component along the CH_2 symmetry axis, the above result indicates that the CH_2 axis must be nearly perpendicular to the surface plane. On the other hand, the CH_2 a-mode is most prominent at $\gamma = 0^\circ$ in the SPS spectra, but vanishes at $\gamma = 90^\circ$. Since excitation of the

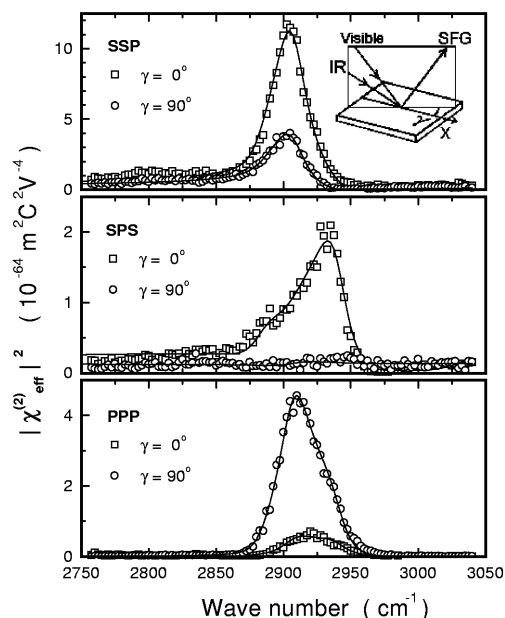


Fig. 3 SFG spectra of a rubbed PVA surface in the CH stretch region for three different polarization combinations: SSP, SPS, and PPP. Solid lines are theoretical fits. The inset defines γ for the azimuthal sample orientation. (After ref. 7.)

a-mode requires an infrared component in the CH_2 plane and perpendicular to the CH_2 axis, this indicates that the CH_2 plane must be nearly perpendicular to the rubbing direction. So the average orientation of the CH_2 groups at the surface is well defined. Knowing that the main chains of PVA must be perpendicular to the CH_2 planes, we can conclude that the main chains should be oriented more or less along the rubbing direction. A quantitative analysis of the SFG spectra allows us to determine not only the average orientation of CH_2 , and hence the main chains, but also an approximate orientational distribution.

In a more qualitative sense, SFG-VS can also be used to study surfaces of complex polymers, for example, polyurethanes (PU) [9]. Polyurethanes are materials useful for biomedical applications in blood contact situation. It has been found that by appending different end groups with different chemical properties to PU molecules, the surface properties of PU can be modified without significantly changing the bulk properties [10]. SFG-VS allows us to prove that the hydrophobic end groups tend to segregate out to the surface despite their small concentration in the bulk, thus drastically modifying the surface properties of PU. For polymers with hydrophilic end groups, the hydrophilic groups tend to remain in the bulk with the surface covered mainly by the PU backbones.

Surface melting of ice

M. Faraday first proposed that there could exist on ice a thin film of liquid water even below the bulk melting temperature [11]. Not until the 1960s was his idea taken seriously [12]. The phenomenon, known as surface melting of ice, appears to be intimately related to many aspects of our modern life, for example, ice sintering, glacier flows, frost heaves, lightning, ozone depletion, and environmental pollution [13]. For this reason, it has been investigated extensively by many techniques. While all experiments seem to confirm that surface melting of ice does exist, the observed surface melting tem-

peratures differ widely. It is possible that different techniques probe different surface properties that respond to surface melting differently.

Being highly surface-specific, SFG-VS is an ideal tool to probe surface melting of ice [14]. However, the technique is more sensitive to orientation of surface molecules and can probe surface melting only via its effect on the orientational motion of the surface molecules. Figure 4 describes the hexagonal ice structure and the PPP-SFG vibrational spectra in the OH stretch region for the ice/vapor interface. The strong peak at $\sim 3200\text{ cm}^{-1}$ originates from OH groups hydrogen-bonded to the neighbors. The narrow peak at 3700 cm^{-1} can be unequivocally assigned to the dangling OH bonds at the surface. For the study of surface melting, we focus on the latter. Figure 5 shows how the peak varies with temperature below the bulk melting temperature. We know that if the ice surface would remain crystalline, the peak position and strength would not have changed appreciably with temperature. But as shown in Fig. 5,

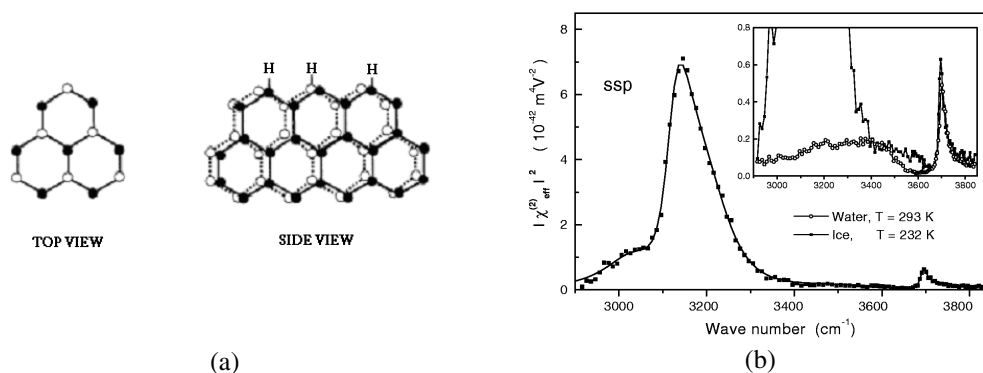


Fig. 4 (a) Top view and side view of the hexagonal hydrogen-bonding structure of ice at the (0001) surface. (b) SFG spectrum of the (0001) surface of ice at 232 K. The inset shows the spectrum of the water surface at 293 K (open symbols) for comparison. (After ref. 14.)

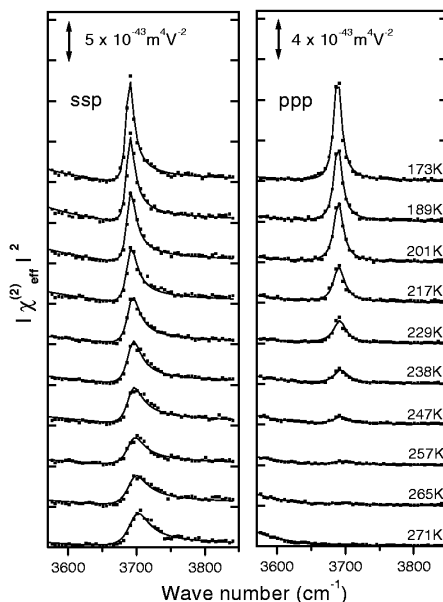


Fig. 5 SFG spectra of the free OH stretch mode for the (0001) surface of ice at various temperature. The polarization combinations are SSP and PPP. (After ref. 14.)

it actually decreases rapidly with increase of temperature above $-70\text{ }^{\circ}\text{C}$, and practically disappears above $-10\text{ }^{\circ}\text{C}$. This decrease in peak strength is due to molecular motion that leads to a broadened orientational distribution of the dangling OH bonds. The result suggests that surface melting of ice has set in near $-70\text{ }^{\circ}\text{C}$. A quantitative analysis of the spectra shows that the orientational order parameter of the dangling OH bonds decreases from 1 (for perfect ordering) around $-70\text{ }^{\circ}\text{C}$ to 0.3 at $0\text{ }^{\circ}\text{C}$.

Ferroelectric ice films

SFG-VS can also be used to probe bulk structures of materials, for example, in distinguishing structure with or without inversion symmetry. We consider here probing of ferroelectric structure of ice as an example [15]. The question whether ice can be ferroelectric has long attracted much attention. It is known that hydrogen-bonding of water molecules to form ice should obey the ice rules [16]: each molecule should donate two protons to two of the tetrahedrally attached neighboring molecules and accept two protons from the other two. This leaves many possible ways to orient water molecules in an ice lattice, giving rise to a residual entropy even at 0 K, and hence discriminating against the occurrence of polar ordering of molecules in ice [17]. Poling by DC electric field to create polar ordering in ice is possible, but requires vacancies in the ice lattice to facilitate poling [18]. Another possible scheme to create polar ordering is via epitaxial growth on a matched surface [15]. This could happen on the Pt(111) surface whose lattice structure matches quite well with the hexagonal face of ice. Since water molecules adsorb on Pt with their oxygen bound to Pt, the first adsorbed water monolayer is polar-oriented. Then, by ice rules, the subsequent adsorbed layers must also be polar-oriented, although at finite temperatures, such a polar ordering could be deterred by thermally generated defects that would break the ice rules. Thus one could expect to find a ferroelectric ice film on Pt(111) with a finite film thickness.

We were able to grow thin films of ferroelectric ice on Pt(111) [15]. SFG-VS is the ideal technique to probe polar ordering in ice. With perfect polar ordering, the spectral intensity should be proportional to the square of the film thickness according to eqs. 2–4. Without polar ordering, the strength is dominated by the surface contribution and therefore is independent of film thickness. Figure 6 depicts a set of SFG spectra in the OH stretch region for different thickness of ice films grown on Pt(111) at 120 K.

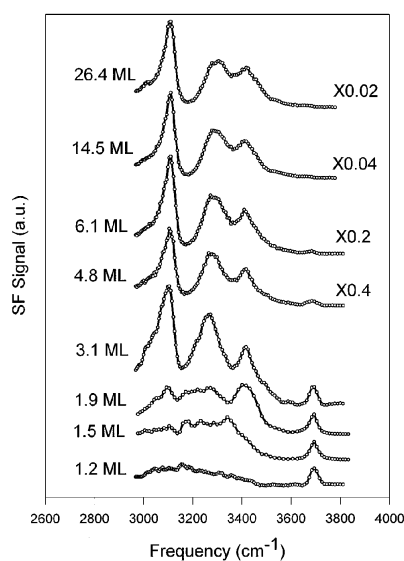


Fig. 6 SFG spectra in the OH stretch region for a set of ice films of different thickness on Pt(111). The polarization combination used is PPP. (After ref. 15.)

Below 3 ML, the spectral features between 3000 and 3600 cm^{-1} changes with film thickness as the interfacial ice structure mismatched from that of Pt makes transition toward the bulk ice structure. The narrow peak at 3700 cm^{-1} is from the dangling OH bonds at the surface and does not change with film thickness. Above 3 ML, the spectral shape remains more or less unchanged, but the spectral strength increases first with square of the film thickness, then shows saturation, and finally reaches a constant at ~ 70 ML. This result is a clear manifestation of the existence of polar ordering in these ice films, although such polar ordering decays away after ~ 70 ML. Quantitative analysis of the spectra shows that the polar ordering decays exponentially away from the surface with a coherent length of ~ 30 ML at 120 K.

Vibrational chirality of chiral liquids

The importance of molecular chirality in chemistry and bioscience has been well recognized [19]. Homochirality of biomolecules in nature is still an unanswered question intimately related to the origin of life. How to measure and interpret molecular chirality has always been a subject of interest to many researchers. Optical circular birefringence, circular dichroism, and Raman optical activity are the commonly employed techniques for probing chirality. All of them are electric-dipole forbidden processes [20], so their sensitivities are relatively low, especially for probing vibrational chirality. As nonlinear optical spectroscopic techniques become more mature, one may ask whether they could also be used as effective probes to study molecular chirality. SFG-VS is an obvious candidate.

A chiral system is intrinsically centro-asymmetric. Therefore, even in a chiral liquid, SFG is electric-dipole allowed. In fact, as pointed out by Giordmaine [21] early in 1965, the only allowed nonvanishing elements of $\chi_{ijk}^{(2)}$ of a chiral liquid are the chiral elements $\chi_{ijk}^{(2)} (i \neq j \neq k) = \chi_C$, which can be used as a measure of the molecular chirality of the liquid. However, conclusive report on the observation of SFG in chiral liquids only appears very recently [22].

Figure 7 shows the SFG vibrational spectra of limone ($\text{CH}_3\text{-C}_6\text{H}_8\text{-C}_3\text{H}_5$) in the CH stretch region obtained by the transmission geometry [22]. The SPP and PSP polarization combinations measure directly the chiral nonlinear susceptibility element χ_C . Since the SFG signal is proportional to $|\chi_C|^2$, the

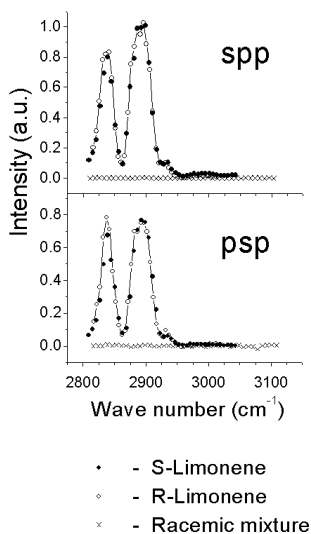


Fig. 7 Chiral SFG spectra of three kinds of limone liquids in the CH stretch range obtained by the transmission geometry using SPP and PSP polarization combinations. (After ref. 22.)

spectra are identical for left- and right-handed limone although χ_C of the two are opposite in sign. On the other hand, the spectra disappear completely for the racemic mixture as expected.

Quantitative evaluation of the spectra, however, finds that $|\chi_C|$ is three orders of magnitude smaller than a typical electric-dipole allowed $\chi^{(2)}$ element. The reason is perhaps obvious. The CH stretch modes observed are associated with CH_x groups that are not chiral if isolated in space. The vibrational chirality they carry is induced by the surrounding chiral arrangement of atoms in the molecule, and is expected to be weak. In addition, theory indicates that the existence of vibrational chirality requires a breakdown of the Born–Oppenheimer approximation for the molecule. Despite the weak signal strength, the result still shows that SFG-VS is promising as an effective tool to probe vibrational chirality.

Doubly resonant SFG spectroscopy

The schematic diagram in Fig. 1a suggests that if ω_1 and ω_2 are both tunable, SFG can experience double resonance (DR) [3]. But the doubly resonant enhancement is possible only if the two resonant transitions are coupled. DR-SFG belongs to the class of two-dimensional spectroscopy that generally allows for more selective spectroscopic studies and probing of intra- and intermolecular coupling in a medium. It has the additional advantage of being highly surface-specific.

In a recent experiment on a monolayer of rhodamine-6G adsorbed on silica, we have successfully demonstrated for the first time infrared-visible DR-SFG as a two-dimensional surface spectroscopic technique [23]. When ω_1 and ω_2 were scanned simultaneously over the S_0 – S_1 electronic transition and the CH stretch vibrational transitions of rhodamine-6G, respectively, doubly resonant enhancement of SFG was observed. It showed an unprecedented surface sensitivity owing to the strong resonant enhancement. From the DR-SFG spectra, relative electron-vibration coupling strengths between different vibrational modes and the S_0 – S_1 electronic resonance of rhodamine-6G were deduced. Although the work is on an adsorbed monolayer, it obviously can be extended to other surfaces or interfaces, including those of neat liquids and solids.

CONCLUSION

SFG-VS has been developed into a very powerful and versatile spectroscopic technique in recent years. It can be highly surface-specific and enables studies of surfaces and interfaces at a molecular level. It can also be useful for studying bulk materials. We present here a few selected examples representing our recent effort in finding unique applications for the technique. There certainly exist many other possible applications yet to be explored. Examples are studies of liquid/liquid, liquid/solid, and biological interfaces, *in situ* investigation of chemical vapor deposition, etching, and reactions, probing surface dynamics, and development of surface microscopy. Further advances in applications of the technique are predictable. The future would be brighter if tunable coherent sources can be easily extended to longer and shorter wavelengths.

ACKNOWLEDGMENT

This work was supported by the Director, Office of Energy Research, Office of Basic Energy Sciences, Materials Science Division of the U.S. Department of Energy under Contract No. DE-AC03-76SF00098.

REFERENCES AND NOTES

1. See, for example: Y. R. Shen. In *Nonlinear Spectroscopy for Molecular Structure Determination*, R. W. Field, E. Hirota, J. P. Maier, S. Tsuchiya (Eds.), Blackwell Science, Oxford (1998).

2. More generally, even for media without inversion symmetry, SFG could be used to probe surfaces or interfaces. Because surface and bulk often have different structural symmetries, selective input/output polarization combinations could be employed to discriminate against the bulk contribution.
3. J. Y. Huang and Y. R. Shen. *Phys. Rev. A* **49**, 3973 (1994).
4. P. Miranda and Y. R. Shen. *J. Chem. Phys. B* **103**, 3292 (1999).
5. Y. L. Yeh, C. Zhang, H. Held, A. M. Mebel, X. Wei, S. H. Lin, Y. R. Shen. *J. Chem. Phys.* **114**, 1837 (2001).
6. D. Zhang, Y. R. Shen, G. A. Somorjai. *Chem. Phys. Lett.* **281**, 394 (1997); D. Kim and Y. R. Shen. *Appl. Phys. Lett.* **74**, 3314 (1999); Z. Chen, R. Ward, Y. Tian, A. A. Eppler, Y. R. Shen, G. A. Somorjai. *J. Phys. Chem. B* **103**, 2935 (1999); K. S. Gautam, A. D. Schwab, A. Dhinojwala, D. Zhang, S. M. Dougal, M. S. Yaganeh. *Phys. Rev. Lett.* **85**, 3854 (2000); K. A. Briggman, J. C. Stephenson, W. E. Wallace, L. J. Richter. *J. Phys. Chem. B* **105**, 2785 (2001).
7. X. Wei, X. Zhuang, S. C. Hong, T. Goto, Y. R. Shen. *Phys. Rev. Lett.* **82**, 4256 (1999).
8. J. M. Geary, J. W. Goodby, A. R. Kmetz, J. S. Patel. *J. Appl. Phys.* **62**, 4100 (1987).
9. Z. Chen, R. Ward, Y. Tian, S. Baldelli, A. Opdahl, Y. R. Shen, G. A. Somorjai. *J. Am. Chem. Soc.* **122**, 10615 (2000).
10. R. S. Ward and K. A. White. U.S. Patent #5589563.
11. M. Faraday. *Athenaeum* 1181, 640 (1850); *Philos. Mag.* **17**, 162 (1859); *Proc. Roy. Soc. London* **10**, 440 (1860).
12. N. H. Fletcher. *Philos. Mag.* **18**, 1287 (1968).
13. J. S. Wettlaufer and J. G. Dash. *Sci. Am.* **282** (2), 34 (2000).
14. X. Wei, P. Miranda, Y. R. Shen. *Phys. Rev. Lett.* **86**, 1554 (2001).
15. X. Su, L. Lianos, Y. R. Shen, G. Somorjai. *Phys. Rev. Lett.* **80**, 1533 (1998).
16. J. D. Bernal and R. H. Fowler. *J. Chem. Phys.* **1**, 515 (1933).
17. L. Pauling. *J. Am. Chem. Soc.* **57**, 2680 (1935); W. F. Giaugue and J. W. Stout. *J. Am. Chem. Soc.* **58**, 1144 (1936).
18. S. M. Jackson and R. W. Whitworth. *J. Chem. Phys.* **103**, 7647 (1995).
19. See, for example: P. Ball. *Designing the Molecular World*, Princeton University Press, Princeton, NJ (1996).
20. See, for example: L. D. Barron. *Molecular Light Scattering and Optical Activity*, Cambridge University Press, Cambridge, UK (1982).
21. J. A. Giordmaine. *Phys. Rev.* **138**, A 1599 (1965).
22. M. A. Belkin, T. A. Kulakov, K.-H. Ernst, L. Yan, Y. R. Shen. *Phys. Rev. Lett.* **85**, 4474 (2000).
23. M. B. Raschke, Y. R. Shen, M. Hayashi, S. H. Lin. To be published.